

Determining the upper limit of Γ_{ee} for the $Y(4260)$

X.H. Mo ^{a*}, G. Li ^{a,b}, C.Z. Yuan ^a, K.L. He ^a, H.M. Hu ^a, J.H. Hu ^{a,c}, P. Wang ^a, Z.Y. Wang ^a

^aInstitute of High Energy Physics, P.O.Box 918, Beijing 100049, China

^bChina Center of Advanced Science and Technology, Beijing 100080, China

^cCollege of Physics and Information Technology, Guangxi Normal University, Guilin 541004, China

By fitting the R values between 3.7 and 5.0 GeV measured by the BES collaboration, the upper limit of the electron width of the newly discovered resonance $Y(4260)$ is determined to be $580 \text{ eV}/c^2$ at 90% C.L. Together with the BaBar measurement on $\Gamma_{ee} \cdot \mathcal{B}(Y(4260) \rightarrow \pi^+ \pi^- J/\psi)$, this implies a large decay width of $Y(4260) \rightarrow \pi^+ \pi^- J/\psi$ final states.

1. Introduction

Recently, in studying the initial state radiation events, $e^+e^- \rightarrow \gamma_{ISR} \pi^+ \pi^- J/\psi$ (γ_{ISR} : initial state radiation photon) with 233 fb^{-1} data collected around $\sqrt{s} = 10.58 \text{ GeV}$, the BaBar Collaboration observed an accumulation of events near $4.26 \text{ GeV}/c^2$ in the invariant-mass spectrum of $\pi^+ \pi^- J/\psi$ [1]. The fit to the mass distribution yields 125 ± 23 events with a mass of $4259 \pm 8_{-6}^{+2} \text{ MeV}/c^2$ and a width of $88 \pm 23_{-4}^{+6} \text{ MeV}/c^2$. In addition, the following product is calculated

$$\begin{aligned} & \Gamma(Y(4260) \rightarrow e^+e^-) \cdot \mathcal{B}(Y(4260) \rightarrow \pi^+ \pi^- J/\psi) \\ &= 5.5 \pm 1.0_{-0.7}^{+0.8} \text{ eV}/c^2. \end{aligned} \quad (1)$$

Since the resonance is produced in initial state radiation from e^+e^- collision, its quantum number $J^{PC} = 1^{--}$. However, this new resonance seems rather different from the known charmonium states with $J^{PC} = 1^{--}$ in the same mass scale, such as $\psi(4040)$, $\psi(4160)$, and $\psi(4415)$. Being well above the $D\bar{D}$ threshold, instead of decaying predominantly into $D^{(*)}\bar{D}^{(*)}$ final states, the $Y(4260)$ shows strong coupling to the $\pi^+ \pi^- J/\psi$ final state. So this new resonance does not seem to be a usual charmonium state. The strange properties exhibited by the $Y(4260)$ have

triggered many theoretical discussions [2]-[12].

One suggestion is that the $Y(4260)$ is the first orbital excitation of a diquark-antidiquark state ($[cs][\bar{c}\bar{s}]$) [2,3]. By virtue of this scheme, the mass of such a state is estimated to be $4.28 \text{ GeV}/c^2$, which is in good agreement with the observation. A crucial prediction of the scheme is that the $Y(4260)$ decays predominantly into $D_s \bar{D}_s$.

Another opinion favors a hybrid explanation [4, 5,6,7]. In the light of the lattice inspired flux-tube model, the calculation shows that the decays of hybrid meson are suppressed to pairs of ground state $1S$ conventional mesons [13,14]. This implies that decays of $Y(4260)$ into $D\bar{D}$, $D_s \bar{D}_s$, and $D_s^* \bar{D}_s^*$ are suppressed whereas $D^* \bar{D}$ and $D_s^* \bar{D}_s$ are small, and $D^{**} \bar{D}$, if above threshold, would dominate (P -wave charmonia are denoted by D^{**}). So it is interesting to search for the possible decay of $Y(4260) \rightarrow D_1(2420) \bar{D}$.

The third interpretation we wish to mention is provided by Ref. [8], which suggests that the $Y(4260)$ is the second most massive state in the charmonium family. The author ascribes the lack of $Y(4260)$ in $e^+e^- \rightarrow$ hadrons to the interference of S - D waves, and also estimates

$$\Gamma(Y(4260) \rightarrow e^+e^-) \simeq 0.2 - 0.35 \text{ keV}/c^2. \quad (2)$$

Besides the above interpretations, there are other kinds of proposals. The lattice study in Ref. [9] suggests that the $Y(4260)$ behaves like a $D_1 \bar{D}$ molecule. In Ref. [10], it is proposed that the new state might be a baryonium, containing

*Supported by National Natural Science Foundation of China (10491302,10491303), 100 Talents Program of CAS (U-25), and the Knowledge Innovation Project of CAS (U-612(IHEP)).

charms, configured as $\Lambda_c\bar{\Lambda}_c$. In Ref. [11], the $Y(4260)$ is considered as a $\rho\text{-}\chi_{c1}$ molecule while in Ref. [12], the $Y(4260)$ is considered as an $\omega\text{-}\chi_{c1}$ molecule. However, all aforementioned speculations need further experimental judgment.

Most recently, CLEOc collected 13.2 pb^{-1} data at $\sqrt{s} = 4.26\text{ GeV}$ and investigated 16 decay modes with charmonium or light hadrons [15], and the channels with more than 3σ statistical significance are $\pi^+\pi^-J/\psi$ (11σ), $\pi^0\pi^0J/\psi$ (5.1σ), and K^+K^-J/ψ (3.7σ). No compelling evidence is found for any other decay modes for the $Y(4260)$, nor for the $\psi(4040)$ and $\psi(4160)$ resonances [15]. These measurements disfavor the $\rho\text{-}\chi_{c1}$ molecular model [11], baryonium model [10], and high charmonium state explanation [8]. So far as other surviving speculations are concerned, such as charmonium hybrid [4,5,6,7], tetraquark model [2,3], $D_1\bar{D}$ molecule suggestion, and $\omega\text{-}\chi_{c1}$ molecule explanation [12], further experimental studies are needed to make more definitive conclusions.

Since the $Y(4260)$ was observed in e^+e^- annihilation, it is expected that it contributes to the total hadronic cross section in e^+e^- annihilation (or the R value, in other words). The most recent such data on R measurements are from the BES experiment [18,19], as shown in Fig. 1 for $E_{c.m.}(=\sqrt{s})$ from 3.7 to 5.0 GeV. If we look in detail within the range from 4.25 to 4.30 GeV (refer to the inset of Fig. 1), it seems there is a bump around 4.27 GeV. Has this structure a connection with the $Y(4260)$? We try to answer this question in this Letter. As there are other resonances nearby, we shall fit the full spectrum between 3.7 to 5.0 GeV in order to get the information on the $Y(4260)$.

2. Fit to the ψ -resonances

The R values [18,19] used in this analysis were measured with the Beijing Spectrometer (BESII), which is a conventional solenoidal detector expounded in Ref. [16]. In the analysis below, the R values are converted into a cross section $\sigma(e^+e^-)$ by multiplying the Born order cross section of $e^+e^- \rightarrow \mu^+\mu^-$. These cross sections are plotted in Fig. 2. There are clear peaks of $\psi(3770)$,

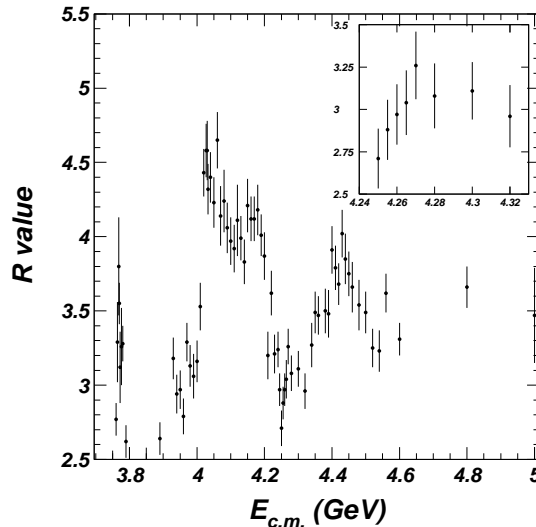


Figure 1. R values for $E_{c.m.}$ from 3.7 to 5.0 GeV measured by the BES collaboration [18,19]. The inset shows the R values in the vicinity of the $Y(4260)$.

$\psi(4040)$, $\psi(4160)$, and $\psi(4415)$. The data points have been used to obtain the parameters of the ψ -resonances [17].

To acquire the resonance parameters, we could simply fit the data set with cross section formula, each resonance with a Breit-Wigner

$$\sigma_j(s) = \frac{12\pi\Gamma_h^j\Gamma_{ee}^j}{[s - (M^j)^2]^2 + (M^j\Gamma_t^j)^2}, \quad (3)$$

where Γ_{ee} , Γ_h , and Γ_t are the mass independent electronic, hadronic and total widths, respectively, for a vector resonance of mass M produced in the head-on collision of e^+ and e^- . Notice that $\Gamma_{ee} \ll \Gamma_t$ in our analysis; the approximation $\Gamma_h \approx \Gamma_t$ is actually adopted hereinafter. The summation of all the cross sections within the range we are studying is

$$\sigma_1(s) = \sum_{j=1}^4 \sigma_j(s), \quad (4)$$

where indices 1, 2, 3, and 4 denote four resonances

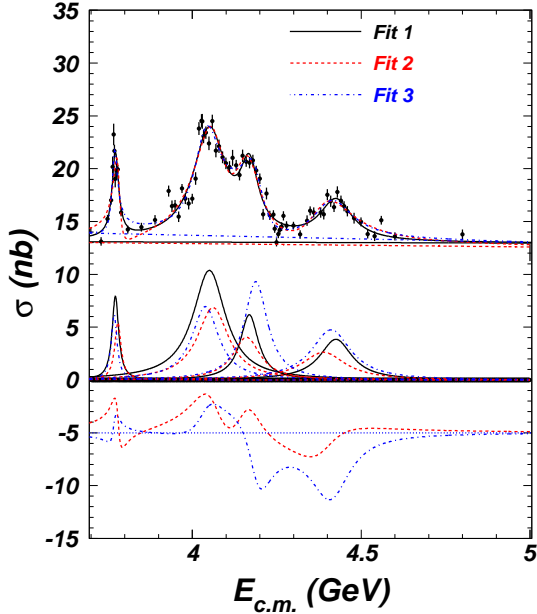


Figure 2. Total hadronic cross section in nb obtained as $\sigma(e^+e^- \rightarrow \text{hadrons}) = R \cdot 86.85/s$ (s in GeV^2) from R values in Refs. [18,19]. Three sets of fit results, Fit 1, Fit 2, and Fit 3 correspond to three cross section forms σ_1 , σ_2 , and σ_3 as described in text. Two interference curves have been moved downward by 5 nb for display purposes; the dashed line at -5 nb corresponds to zero cross section in the fit.

$\psi(3770)$, $\psi(4040)$, $\psi(4160)$, and $\psi(4415)$, respectively.

In the ψ -family resonance region, if we assume that all two-body $D^{(*)}\bar{D}^{(*)}$ states are decay products of resonance, and not produced directly in continuum, we could therefore treat resonance and continuum incoherently. Nevertheless, for the four wide resonances, they are close and are expected to have some same decay final states, there must be interference between any two of the resonances. Therefore the amplitudes corresponding to each resonance, with the following

form

$$T_j(s) = \frac{\sqrt{12\pi\Gamma_h^j\Gamma_{ee}^j}}{[s - (M^j)^2] + iM^j\Gamma_t^j}, \quad (5)$$

have to be added coherently to give the total amplitude that, once squared, will contain interferences of the type $\Re T_i^* T_j$. If the resonances are quite broad, the interference effect can also distort the resonance shape, the width might appear broader or narrower, and the position of the peak can be displaced as well. In this case, the total cross section is

$$\sigma_2(s) = \left| \sum_{j=1}^4 T_j(s) \right|^2, \quad (6)$$

where $T_j(s)$ is given in Eq. (5).

So far as the amplitude is concerned, in principle, there are presumably relative phases between different amplitudes besides the phase due to complex Breit-Wigner formula itself. So a more comprehensive total cross section would be the summation of amplitudes together with an additional phase, viz.

$$\sigma_3(s) = \left| \sum_{j=1}^4 T_j(s) e^{-i\phi_j} \right|^2. \quad (7)$$

Since what we actually obtain is the squared modulus of amplitudes, only three relative phases could be detected in practice.

The standard chi-square estimator is constructed as follows

$$\chi^2 = \sum_{j=1}^n \frac{(\sigma^{exp}(s_j) - \sigma^{the}(s_j))^2}{(\Delta\sigma^{exp}(s_j))^2}, \quad (8)$$

where $\sigma^{exp}(s_j)$ indicates the experimentally measured cross section at the j -th energy point, while $\sigma^{the}(s_j)$ is the corresponding theoretical expectation at this energy point, which is composed of two parts

$$\sigma^{the}(s_j) = \sigma^{res}(s_j) + \sigma^{con}(s_j), \quad (9)$$

where σ^{con} denotes the contribution from continuum. Since there is little evidence in the data for

any substantial variation of the continuum background within the studied energy region, we parameterize the continuum cross section with a linear function

$$\sigma_{bg}(s) = A + B(\sqrt{s} - 3.700), (s \text{ in GeV}^2), \quad (10)$$

as has been used in Ref. [17]. Here we consider the continuum contribution as the background for measurement of resonance parameters, that is $\sigma_{bg}(s) = \sigma^{con}(s)$.

In Eq. (9) σ^{res} denotes the contribution from resonances. The fit results are displayed in Fig. 2 where Fit 1, Fit 2, and Fit 3 correspond to the three cross section forms σ_1 , σ_2 , and σ_3 , as expressed in Eqs. (4), (6), and (7), respectively. Although the synthetic curves for three fits are almost the same, as we expected, the interference effect deforms each resonance significantly, according to Fig. 2, $\psi(3770)$ and $\psi(4040)$ become narrower while $\psi(4160)$ and $\psi(4415)$ become wider when interference effects are included. There exist constructive interferences as well as destructive ones, and the interference behaviors for amplitudes with and without extra phases are also very distinct. The fit results indicate that Γ_{ee} is very sensitive to the fit strategy, and the largest difference between various amalgamation strategies could reach 50%.

Since $\psi(3770)$, $\psi(4040)$, $\psi(4160)$, and $\psi(4415)$ have similar decay features, that is, all decay dominantly to $D^{(*)}\bar{D}^{(*)}$ final states, we prefer the synthetic scheme of amplitude with phase which takes into account all possible interactions between resonances.

So far as the $Y(4260)$ is concerned, the study of the BaBar Collaboration [1] implies that this new state may not be a common charmonium state, whose decay feature is rather distinctive from other ψ -family members, and this also obtains support from recent CLEOc measurements [15]. So it is favorable to perform the incoherent addition for the contribution of the $Y(4260)$ to the total cross sections in Eqs. (4), (6), or (7).

In addition, two other effects should be taken into account. First, there are theoretical arguments in some references [3,4,5,6] that the $Y(4260)$ may be due to a threshold effect just as the $\psi(3770)$, so the width of the $Y(4260)$ could

be energy dependent as follows:

$$\Gamma_{DD}(s) = \bar{\Gamma}_{DD} \cdot \theta(\sqrt{s} - 2m_{D_s^{*\pm}}) \times \frac{p_{D_s^{*\pm}}^3}{1 + (rp_{D_s^{*\pm}})^2} \cdot \frac{1 + (r\bar{p}_{D_s^{*\pm}})^2}{\bar{p}_{D_s^{*\pm}}^3}. \quad (11)$$

Here the subscript “ DD ” explicitly denotes the threshold effect, $\bar{\Gamma}_{DD} = \Gamma_{DD}(M^2)$, r is the classical interaction radius, p is the $D_s^{*\pm}$ momentum,

$$p_{D_s^{*\pm}} = \frac{1}{2}\sqrt{s - 4m_{D_s^{*\pm}}^2};$$

and \bar{p} is the $D_s^{*\pm}$ momentum at resonance peak, viz.

$$\bar{p}_{D_s^{*\pm}} \equiv p_{D_s^{*\pm}} \Big|_{\sqrt{s}=M} = \frac{1}{2}\sqrt{M^2 - 4m_{D_s^{*\pm}}^2}.$$

Second, the $Y(4260)$ has been observed decaying into the $\pi^+\pi^-J/\psi$ final state and this kind of decay can be expressed by the amplitude with the form of Eq. (5) which is different from that of the decay into $D_s^{*+}D_s^{*-}$ with threshold effect. Furthermore, although the present data display the distinctive feature of the $Y(4260)$ from other charmonium resonances, some connections presumably exist which could lead to the interference effects of the $Y(4260)$ with other ψ -family members. With all these considerations in mind, we split the amplitude of the $Y(4260)$ into two parts. One is the amplitude of the threshold part, which is defined as follows:

$$T_{DD}(s) = \frac{\sqrt{12\pi\Gamma_{DD}(s)\Gamma_{ee}}}{(s - M^2) + iM\Gamma_t(s)}, \quad (12)$$

where the total decay width is defined as the summation of two parts :

$$\Gamma_t(s) = \Gamma_{DD}(s) + \Gamma_{non}.$$

Here the first term is the energy dependent partial decay width for the threshold part while the second term is the energy independent partial decay width for the non-threshold part (denoted by Γ_{non}). We introduce a factor f to indicate the ratio of $\Gamma_{DD}(s)$ to $\Gamma_t(s)$ at the resonance peak, that is

$$f = \frac{\Gamma_{DD}(M^2)}{\Gamma_t(M^2)} = \frac{\bar{\Gamma}_{DD}}{\bar{\Gamma}_t}.$$

Notice the energy independence of Γ_{non} , we have $\Gamma_{non} = (1 - f)\bar{\Gamma}_t$, then

$$\Gamma_t(s) = \Gamma_{DD}(s) + (1 - f)\bar{\Gamma}_t .$$

In this case, the amplitude of the non-threshold part is given by the following expression

$$T(s) = \frac{\sqrt{12\pi(1 - f)\bar{\Gamma}_t\Gamma_{ee}}}{(s - M^2) + iM\Gamma_t(s)} . \quad (13)$$

Without the knowledge of f , we first set $f = 0.5$ in the study in Sect. 3 and leave the variation effect of f to Sect. 4.

By virtue of the above discussion, the synthetic cross section within the region studied takes the following form

$$\sigma(s) = \left| \sum_{j=1}^4 T_j(s)e^{-i\phi_j} + T(s)e^{-i\phi} \right|^2 + |T_{DD}(s)|^2 . \quad (14)$$

Under such a scheme, the upper limit of the production of the $Y(4260)$ in e^+e^- annihilation is determined, as expounded in the following section.

3. Determination of Γ_{ee} of the $Y(4260)$

Various fits to the data tell us that with limited knowledge on the nature of the resonances and comparatively meager data, we could only determine the Γ_{ee} of the $Y(4260)$ by a scan method. Specifically, we fix the mass of the $Y(4260)$ at $4.259 \text{ GeV}/c^2$ measured by the BaBar Collaboration [1], and scan over the $\Gamma_t \in (20, 180) \text{ MeV}/c^2$ ($8 \text{ MeV}/c^2$ step) and $\Gamma_{ee} \in (0, 1000) \text{ eV}/c^2$ ($10 \text{ eV}/c^2$ step) parameter space. In order to avoid some grotesque fit results due to random effect of the $Y(4260)$ on the resonances nearby, in the scan procedure, the lower and upper bounds of the masses (total widths) are fixed to be 4100 and $4220 \text{ MeV}/c^2$ (30 and $250 \text{ MeV}/c^2$) and 4350 and $4500 \text{ MeV}/c^2$ (30 and $300 \text{ MeV}/c^2$) for $\psi(4160)$ and $\psi(4415)$, respectively.

For each pair of $\Gamma_{ee}^i (= [i \times 10] \text{ eV}/c^2)$ and $\Gamma_t^j (= [20 + j \times 8] \text{ MeV}/c^2)$, fitting the R data with the χ^2 determined from Eq. (8), we obtain

a best estimated χ^2 as a function of the Γ_{ee}^i and Γ_t^j , or equivalently a relative likelihood, viz.

$$\mathcal{L}_r(\Gamma_{ee}^i, \Gamma_t^j) = \exp\left(-\frac{1}{2}\chi^2(\Gamma_{ee}^i, \Gamma_t^j)\right) . \quad (15)$$

Instead of using this \mathcal{L}_r directly, we further construct a weighted likelihood as follows

$$\mathcal{L}_w(\Gamma_{ee}^i, \Gamma_t^j) = f_N \cdot \mathcal{L}_r(\Gamma_{ee}^i, \Gamma_t^j) \times \frac{1}{\sqrt{2\pi}\sigma_{\Gamma_t}} \exp\left(-\frac{(\Gamma_t^j - \Gamma_t)^2}{\sigma_{\Gamma_t}^2}\right) , \quad (16)$$

where f_N is an arbitrary normalization factor and the Gaussian term indicates that the possible total width (Γ_t^j) of the $Y(4260)$ is considered to distribute as a Gaussian with the mean value $\Gamma_t = 88 \text{ MeV}/c^2$ and the standard deviation $\sigma_{\Gamma_t} = 23.8 \text{ MeV}/c^2$, which have been determined by the BaBar Collaboration [1]. The weighted likelihood (\mathcal{L}_w) as a function of the Γ_{ee}^i and Γ_t^j of the $Y(4260)$ is shown in Fig. 3(a). Summing $\mathcal{L}_w(\Gamma_{ee}^i, \Gamma_t^j)$ with respect to Γ_t^j , we obtain the variation of \mathcal{L}_w versus Γ_{ee} as shown in Fig. 3(b). The integral of the likelihood curve gives the upper limit of Γ_{ee} of the $Y(4260)$ at 90% confidence level (C.L.):

$$\Gamma_{ee}^{Y(4260)} < 420 \text{ eV}/c^2 . \quad (17)$$

By virtue of Fig. 3(a), we sum up $\mathcal{L}_w(\Gamma_{ee}^i, \Gamma_t^j)$ with respect to Γ_{ee}^i to 90% fraction of the total area then obtain the upper limit of $\Gamma_{ee}^{Y(4260)}$ at 90% C.L. for each $\Gamma_t^{Y(4260)}$. So we obtain the variation of the upper limit of Γ_{ee} versus Γ_t as shown in Fig. 4. All the points are almost in a straight line, which indicates the ratio of the two quantities, or the upper limit of the branching fraction of $Y(4260) \rightarrow e^+e^-$ does not depend on the total width. Taking the slope of the solid line in Fig. 4, we get

$$\mathcal{B}(Y(4260) \rightarrow e^+e^-) < 4.6 \times 10^{-6} ,$$

at 90% C.L.

4. Other possibilities

Although it is reasonable to treat all the ψ -resonances coherently as we once mentioned in

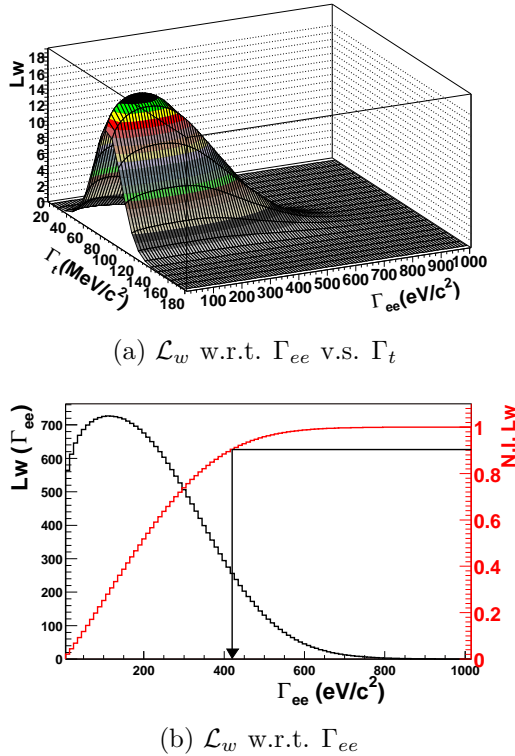


Figure 3. The weighted likelihood (\mathcal{L}_w) distribution with respect to (w.r.t.) Γ_{ee} and Γ_t (a); and to Γ_{ee} with Γ_t integrated (b). The “N.I.” in (b) indicates normalized integral value for \mathcal{L}_w .

Sect. 2, one may argue that other possibilities could exist since there is limited information about the properties of these ψ -resonances. Thereby it’s better to take a variety of effects into consideration.

First, there are three schemes for summation of ψ resonances in this analysis: through cross sections, amplitudes, or amplitudes together with relative phases, as discussed in Sect. 2, the corresponding results are $\Gamma_{ee} < 30, 10, 420 \text{ eV}/c^2$ at 90% C.L. respectively, where the last one has been given in the previous section.

Second, we consider the effect of different background shapes in the fit. In Sect. 2, we adopt the

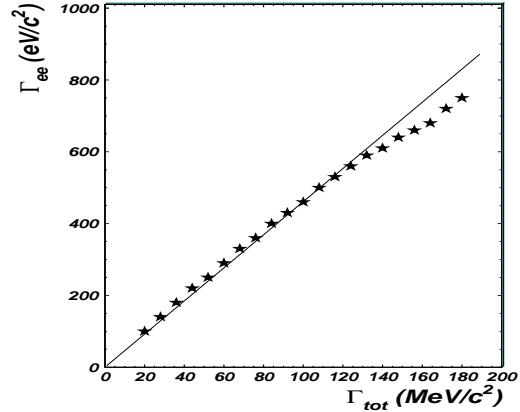


Figure 4. The variation of the upper limit of Γ_{ee} at 90% C.L. with respect to Γ_t . The slope of the solid line denotes the averaged ratio $\Gamma_{ee}/\Gamma_t = 4.6 \times 10^{-6}$.

first order polynomial to depict the background, nevertheless, higher order polynomial can be used to delineate the background as well.

In addition, we notice one background shape once adopted by DASP group, who tried to take into account the threshold effect of the charmed mesons [20],

$$\sigma_{dasp} = \sigma_{e^+e^- \rightarrow \mu^+\mu^-} \cdot (A_0 + \sum_{j=1}^6 A_j \beta_j^3 F^2), \quad (18)$$

with

$$F = \frac{1}{1 - s/(3.1 \text{ GeV})^2}, \quad (19)$$

where A_0 describes the contribution from continuum; j ranging from 1 to 6 indicates the $D\bar{D}$, $D\bar{D}^*$, $D^*\bar{D}^*$, $D_s\bar{D}_s$, $D_s\bar{D}_s^*$, $D_s^*\bar{D}_s^*$ thresholds, respectively. A_j are free parameters²; β_j are the velocities of the relevant particles; and F is a oversimplified form factor defined above.

The fit results show that the effect of polynomial background is at the same level with or

²It should be noticed that since the $D_s^*\bar{D}_s^*$ threshold has been taken into account in description of the $Y(4260)$, the parameter A_6 is set to be zero in the corresponding fit.

smaller than that of the DASP background, so as an estimation, we adopt the linear and the DASP backgrounds as two typical cases for background description. Comparing with those of linear background fit, the results of DASP background fit for three summation schemes of ψ resonances are $\Gamma_{ee} < 50, 30, 250 \text{ eV}/c^2$ at 90% C.L. respectively,

Last, we also consider the possible effect of the fraction f on the measured Γ_{ee} of the $Y(4260)$. Our fits indicate that with the increasing of factor f the upper limit of Γ_{ee} decreases and *vice versa*. The upper limit for Γ_{ee} varies from 580 to 280 eV/c^2 when f changes from 0.3 to 0.7.

Taking all the aforementioned possibilities into account, we adopt the most conservative result as our final estimation, that is

$$\Gamma_{ee}^{Y(4260)} < 580 \text{ eV}/c^2, \quad (20)$$

at 90% C.L.

5. Discussion

According to our study, the conservative estimation for the upper limit of Γ_{ee} of the $Y(4260)$ is about 580 eV/c^2 at 90% C.L., which is almost two times larger than the estimation presented in Eq. (2).

Utilizing our upper limit $\Gamma_{ee} < 580 \text{ eV}/c^2$ for the $Y(4260)$, together with the relation of Eq. (1), we obtain the lower limit of the branching fraction at 90% C.L. to be

$$\mathcal{B}(Y(4260) \rightarrow \pi^+\pi^-J/\psi) > 0.58\% .$$

This means that the partial width $\Gamma(Y(4260) \rightarrow \pi^+\pi^-J/\psi) \geq 508 \text{ keV}/c^2$ at 90% C.L., which is much larger than the corresponding partial widths of ψ' (89.1 keV/c^2) [21] and ψ'' (44.6 keV/c^2) [21,22].

CLEOc measured the cross section for $\pi^+\pi^-J/\psi$ channel to be 58 pb^{-1} [15], which is consistent with the BaBar result, 50 pb^{-1} [1]. As an estimation, we regard the central value calculated in Eq. (1) to be the same for CLEOc and BaBar, but adopt the improved accuracy provided by CLEOc, then we can obtain the following lower limits at 90% C.L.

$$\mathcal{B}(Y(4260) \rightarrow \pi^+\pi^-J/\psi) > 0.6\% ,$$

$$\begin{aligned} \mathcal{B}(Y(4260) \rightarrow \pi^0\pi^0J/\psi) &> 0.2\% , \\ \mathcal{B}(Y(4260) \rightarrow K^+K^-J/\psi) &> 0.1\% , \end{aligned}$$

and

$$\mathcal{B}(Y(4260) \rightarrow XJ/\psi) > 1.3\% ,$$

where X denotes $\pi^+\pi^-$ (37), $\pi^0\pi^0$ (8), K^+K^- (3), η (5), π^0 (1), η' (0), $\pi^+\pi^-\pi^0$ (0), and $\eta\eta$ (1). Here the numbers of the observed events by CLEOc are presented in parentheses.

As we notice up to now only results on hidden-charm final states were reported about the $Y(4260)$; measurements involving open-charm are anxiously awaited to confirm existing speculations or provide clues for further theoretical inquiry. In addition, more accurate Γ_{ee} is still needed for a better understanding of the nature of the $Y(4260)$.

Acknowledgments

We would like to thank Dr. H.B. Li for friendly discussion.

REFERENCES

1. BaBar Collaboration, B. Aubert *et al.*, Phys. Rev. Lett. **95** (2005) 142001.
2. D. Ebert, R.N. Faustov, and V.O. Galkin, hep-ph/0512230. Phys. Lett. B **634** (2006) 214.
3. L. Maiani *et al.*, Phys. Rev. D **72** (2005) 031502.
4. S.L. Zhu, Phys. Lett. B **625** (2005) 212.
5. E. Kou and O. Pene, Phys. Lett. B **631** (2005) 164.
6. F.E. Close and P.R. Page, Phys. Lett. B **628** (2005) 215.
7. X.Q. Luo and Y. Liu, hep-lat/0512044.
8. F. J. Llanes-Estrada, Phys. Rev. D **72** (2005) 031503.
9. T.-W. Chiu and T.H. Hsieh (TWQCD Collaboration), Phys. Rev. D **73** (2006) 094510.
10. C.F. Qiao, hep-ph/0510228.
11. X. Liu, X.Q. Zeng and X. Q. Li, Phys. Rev. D **72** (2005) 054023.
12. C.Z. Yuan, P. Wang and X.H. Mo, Phys. Lett. B **634** (2006) 399.

13. N. Isgur and J. Paton, Phys. Rev. D **31** (1985) 2910; N. Isgur, R. Kokoski and J. Paton, Phys. Rev. Lett. **54** (1985) 869.
14. F.E. Close and P.R. Page, Nucl. Phys. B **443** (1995) 233.
15. CLEO Collaboration, T.E. Coan *et al.*, Phys. Rev. Lett. **96** (2006) 162003.
16. BES Collaboration, J. Z. Bai *et al.*, Nucl. Instrum. Methods A **344** (1994) 319; Nucl. Instrum. Methods A **458** (2001) 627.
17. K.K. Seth, Phys. Rev. D **72** (2005) 017501.
18. BES Collaboration, J. Z. Bai *et al.*, Phys. Rev. Lett. **84** (2000) 594.
19. BES Collaboration, J. Z. Bai *et al.*, Phys. Rev. Lett. **88** (2002) 101802.
20. DASP Collaboration, R. Brandelik *et al.*, Phys. Lett. B **76** (1978) 361.
21. Particle Data Group, S. Eidelman *et al.*, Phys. Lett. B **592** (2004) 1.
22. CLEO Collaboration, N.E. Adam *et al.*, Phys. Rev. Lett. **96** (2006) 082004.